Advances in Ophthalmology Practice and Research 4 (2024) 15–22

Contents lists available at ScienceDirect

Advances in Ophthalmology Practice and Research

journal homepage: www.journals.elsevier.com/advances-in-ophthalmology-practice-and-research

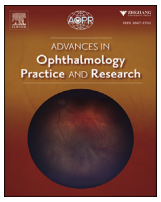

Letter to the Editor

A two-year longitudinal observational study of the peripapillary microvasculature in pediatric type 1 diabetes mellitus patients without visual impairment or diabetic retinopathy

Dear Editor,

Our research embarked on a detailed investigation of the peripapillary microvasculature in pediatric Type 1 Diabetes Mellitus (T1DM) patients, a demographic often overlooked in diabetic retinopathy research. Over the course of two years, we meticulously monitored these patients using Optical Coherence Tomography Angiography (OCTA). Our results revealed significant changes in the peripapillary microvasculature, indicating early microvascular impairment that could precede diabetic retinopathy (Fig. 1).

1. Introduction

Approximately 5 million children worldwide have type 1 diabetes mellitus (T1DM), and this number increases by 80000 people per year.[1] Diabetic children have a younger age of onset and a longer survival period than adult DM patients; almost all of them develop diabetic retinopathy (DR) by the time their DM duration reaches 20 years. DR is the most common microvascular complication in DM patients and the leading cause of blindness and vision loss in working-age people.[2,3] DR causes fundus hemorrhage, macular edema, neurodegeneration and a series of ocular complications, which significantly harm patients' quality of life and increase the burden on society.[4]

Recently, there has been increasing evidence of neurodegeneration preceding microcirculatory deterioration, making DR more than a simple microvascular disease.[5–7] DM patients without clinical signs of DR already had glial cell apoptosis and a thinner retinal nerve fiber layer (RNFL) thickness.[8] Zhang et al.[9] reported that the decrease in peripapillary vessel density occurs earlier than the decline in RNFL thickness among type 2 DM patients without clinical signs of DR, and they speculated that peripapillary microvascular abnormalities in the peripapillary region may affect the normal metabolism of neurons and eventually aggravate the process of DR. Previous studies reported that adults and children with DM had lower macular and peripapillary vessel density than healthy individuals, which held true regardless of whether the DM patients presented clinical signs of DR.[10,11] In 2018, our research group established the Shanghai Children and Adolescent Diabetes Eye (SCADE) study cohort and began a case–control study,[12] which compared the superficial capillary plexus between T1DM children without DR and healthy children. The case–control study revealed that T1DM children had reduced vessel density in the macular area and no significant difference in the peripapillary area compared with healthy children, indicating that the participants with short diabetes durations were still in the early stage of preclinical DR. The longitudinal alterations in peripapillary microcirculation among DM children without DR are meaningful; in this manner, the relationship between peripapillary microvascular abnormalities and preclinical DR progression could be revealed, and metrics for detecting and monitoring the preclinical DR can be discovered. To date, longitudinal observational studies of the peripapillary microcirculation and microvasculature among T1DM children have not been conducted. At present, direct observation of retinal vasculature has become extremely convenient due to the novel noninvasive technique known as optical coherence tomography angiography (OCTA).[13] Previous OCTA studies usually employed only vessel density to describe the blood flow in the retina. However, RK Wang, using an optical microangiography (OMAG) algorithm, developed a series of quantitative parameters that comprehensively reflect the retinal microcirculation and microvasculature.[14] This study was designed to observe longitudinal alterations in the peripapillary microcirculation and microvasculature through OCTA among T1DM children from the SCADE cohort for 2 years. We used the following quantitative parameters to describe the superficial capillary plexus (SCP) and the deep capillary plexus (DCP) in the peripapillary area: vessel diameter index (VDI), vessel area density (VAD), vessel skeleton density (VSD), vessel perimeter index (VPI), vessel complexity index (VCI), flow impairment region (FIR) and flux index (FI). This study aimed to provide new information for the future prevention and treatment of DR in children and adolescents.

2. Materials and methods

This was a 2-year longitudinal observational study. The participants were children with T1DM who belonged to the SCADE cohort (clinicaltrials.gov identifier: NCT03665090) in January 2019 and returned for follow-up in January 2021 at Children's Hospital affiliated with Fudan University in Shanghai and Shanghai Eye Hospital. This study conformed to the guidelines presented in the Declaration of Helsinki. After the participants' guardian completed a written consent form, the participants' examinations were performed with the accompaniment of their guardians.

2.1. Patient selection

The inclusion criteria were as follows: (1) diagnosis of T1DM (according to the World Health Organization diagnostic criteria)[15]; (2) age under 18 years; (3) ability to cooperate in all examinations in this study; (4) best-corrected visual acuity no less than 20/25 in both eyes; and (5) no refractive medium opacity. The exclusion criteria were as follows: (1) diagnosis of DR (based on the international DM classification criteria)[16]; (2) presence of eye diseases that may hinder OCTA examination, such as

https://doi.org/10.1016/j.aopr.2024.01.001
Received 29 August 2023; Received in revised form 9 January 2024; Accepted 9 January 2024
Available online 12 January 2024

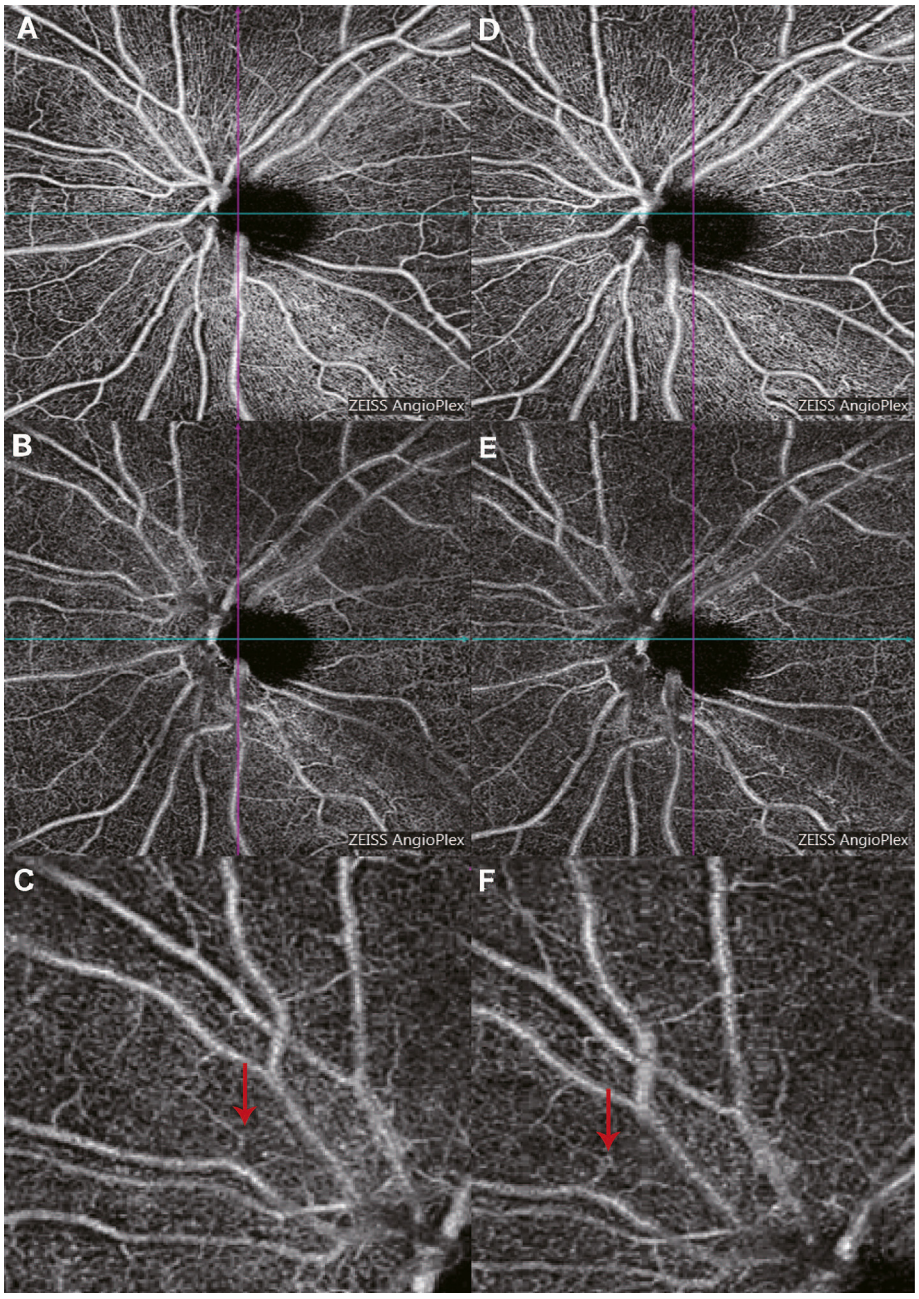

Fig. 1. Typical change of the peripapillary blood circulation after a two-year follow-up. (A-C) Peripapillary OCTA images (6mm * 6mm, OCTA scans) acquired in 2019. (D-F) Peripapillary OCTA images (6mm * 6mm, OCTA scans) acquired in 2021. (A) and (D) shows the superficial capillary plexus, (B) and (E) shows the deep capillary plexus. (C) and (F) are the magnification picture of partial deep capillary plexus, the red arrows indicate a vessel with normal morphology in 2019 showed some tortuosity in 2021.

eyelid disease or strabismus; (3) presence of eye diseases that may induce retinal vasculature alterations, such as macular disease and glaucoma; (4) history of eye injuries or surgeries; and (5) systemic diseases other than DM.

2.2. Eye examination and acquisition of OCTA images

Comprehensive eye examinations included the following: (1) Subjective best-corrected visual acuity and refraction were measured under full mydriasis with cyclopentolate (1 %, Alcon, administered 3 times at 5-min intervals). A log MAR visual acuity chart was used. Refraction was measured by an automatic refractometer (KR-8900, Topcon, JAPAN). (2) Examinations of the eyelid, conjunctiva, cornea, anterior segment, iris, pupil, and lens were performed with a slit lamp (SL130, Zeiss, Germany), and fundus examination was performed with a noncontact lens (90D, Ocular, US). (3) Fundus photography centered on the optic nerve head and macula was performed with a digital fundus camera (AFC-210, NIDEK, Tokyo, JAPAN). (4) Intraocular pressure was examined with a noncontact tonometer (NT-530P, NIDEK, Tokyo, JAPAN). (5) Axial length, anterior chamber depth, cornea thickness, cornea diameter and lens thickness were measured with an IOL Master 700 (Carl Zeiss Meditec, Dublin, CA). (6) SS-OCT (Triton, Topcon, Tokyo, JAPAN) was used for examination of the posterior fundus. (7) OCTA examination (Cirrus HD-OCT 5000 angiography system, Carl Zeiss Meditec, Inc.) was performed with a 6 mm * 6 mm scan pattern centered on the optic nerve head. After the acquisition was finished, the built-in software of the Cirrus 5000 system automatically segmented the retina tissues into the SCP and the DCP. The SCP ranges from 3 μm beneath the inner limiting membrane to 15 μm beneath the inner plexiform layer. The DCP ranges from 15 μm to 70 μm beneath the inner plexiform layer. The OCTA images of the DCP were processed by the built-in projection removal tool to clear the projection of the above large vessels. When OCTA images had low signal intensity (less than 8/10) or contained overlap or artifacts, they were disqualified and excluded from the database. The analysis area

was an annular zone bordered by two rings centered on the optic disc: the inner ring (a circle with a diameter of 1 mm) and the outer ring (a circle with a diameter of 6 mm). The quantitative analysis process was performed using the OMAG algorithm in MATLAB (R2020a, MathWorks, Inc., Natick, MA, USA). The superior, inferior, temporal, and nasal quadrants were analyzed separately.

2.3. Blood circulation indices

The quantitative blood circulation indices calculated by the OMAG algorithm are as follows[14]: (1) The VDI is calculated by using both the vessel area map and the skeletonized vessel map to find the average vessel caliber; the larger the VDI, the larger the average vessel caliber is. (2) VAD is calculated as a unitless ratio of the total image area occupied by the vasculature to the total image area in the binary vessel maps; an increase in VAD indicates an expansion of the blood flow area. (3) VSD is calculated as the ratio of the length occupied by the blood vessels to the total area in the skeletonized vessel map; an increase in VSD indicates an increase in the total quantity of blood vessels. (4) The VPI is calculated using the vessel perimeter map as the ratio of the vessel perimeter to the total area of the OCTA image; it incorporates both the length and the diameter and is similar to VAD. (5) The VCI is calculated using both the vessel perimeter map and the vessel area map; it is used to describe vascular tortuosity, and its value increases when vessels show more chaos and morphological abnormalities. (6) The FIR represents the size of the area with impaired blood flow. (7) The FI is defined as the total number of particles across the imaging voxel cross-section per unit time.

2.4. Statistical analysis

All data analyses were performed by SAS 9.4 (Cary, NC). This study selected the participants' left eyes for statistical analysis. All measurement data are described as the mean ± standard deviation, and all enumeration data are described as frequencies and percentages. All measurement data were tested for normality using the Kolmogorov–Smirnov test. As for the comparison between the baseline values in 2019 and the follow-up values in 2021, variables that followed the normal distribution were compared using a paired *t*-test, and variables with nonnormal distributions were compared by the Wilcoxon rank-sum test. The relationships between the relative changes in the blood circulation indices (change value/baseline value) and the individual demographic and ocular parameters in Table 1 were studied through Pearson correlation analysis, and the statistically significant parameters were selected for further regression analysis. In the multiple regression analysis, the relative changes in the blood circulation indices were selected as the dependent variables, and the statistically significant parameters as described above were selected as independent variables. $P < 0.05$ indicates statistical significance.

3. Results

Forty children in the SCADE cohort presented for examinations in both 2019 and 2021; of these children, 10 were excluded due to poor image quality. The results of the physical examinations and ocular examinations of all participants are shown in Table 1. Of the 30 enrolled participants, 11 (36.67%) were males. All had a best-corrected visual acuity of no less than 20/25. As of 2019, the average age of all participants was 10.93 ± 2.78 years, and the average duration of diabetes was 5.43 ± 2.67 years. During the 2-year follow-up period, all participants underwent repeated slit-lamp examination (assisted by a noncontact 90 D lens), fundus photography, and SS-OCT; in these examinations, no participant was found to present clinical signs of DR, including retinal angiographic abnormalities, fundus hemorrhage and other retinal microvascular anomalies, which indicated that the subjects in this study were still in a relatively early stage of preclinical DR.

Table 1
Basic and ocular parameters of all participants.

	2019 N = 30	2021 N = 30
Basic parameters		
Age, years	10.93 ± 2.78	12.93 ± 2.78
Gender, %	11 Males, 36.67%	
DM duration, years	5.43 ± 2.67	7.43 ± 2.67
HbA1c%	7.08 ± 1.76	7.91 ± 1.54
Systolic pressure, mmHg	110.04 ± 14.30	114.60 ± 14.47
Diastolic pressure, mmHg	71.79 ± 12.09	66.10 ± 10.94
Height, m	1.47 ± 0.17	1.57 ± 0.13
Weight, kg	42.61 ± 14.01	51.60 ± 13.07
BMI, kg/m^2	19.08 ± 2.44	20.55 ± 2.47
Ocular parameters		
SER, diopter	−1.65 ± 2.44	−2.60 ± 2.62
BCVA	−0.01 ± 0.04	0.003 ± 0.02
IOP, mmHg	16.01 ± 2.28	15.52 ± 3.38
Cornea endothelium count	3074.14 ± 296.40	2979.57 ± 433.64
Cornea thickness, μm	557.52 ± 26.17	543.37 ± 35.83
White-to-white, mm	11.96 ± 0.42	9.48 ± 2.23
Axial length, mm	23.97 ± 1.04	24.51 ± 1.04
Anterior chamber depth, mm	3.19 ± 0.29	3.72 ± 0.24
Lens thickness, mm	3.48 ± 0.21	3.45 ± 0.18
With DR, 0%	0, 0%	0, 0%

DM = diabetes mellitus; HbA1c = hemoglobin A1c; BMI = body mass index; SER = spherical equivalent refraction; BCVA = best-corrected visual acuity; IOP = intraocular pressure; DR = diabetic retinopathy.

In the SCP, some of the peripapillary blood circulation indices significantly changed at follow-up compared with the baseline (Table 2). The VDI showed a tendency to increase. The inferior and nasal VDI significantly increased, indicating that the average vessel caliber increased in these 2 quadrants. There was no significant change in the VDI of other quadrants. The VAD showed a tendency to decrease. The superior VAD significantly decreased, indicating that the superior quadrant had a reduced blood flow area. The VAD of the other quadrants did not show a statistically significant change. The VSD showed a tendency to decrease. The VSD of the nasal, superior, and inferior quadrants decreased significantly, indicating that the numbers of blood vessels in these quadrants dropped. There was no obvious change in the VSD of the temporal quadrant. VPI also showed a tendency to decrease. The VPI of the superior and nasal quadrants decreased significantly, indicating that there was a decrease in the blood flow area. The VPI values of the other quadrants did not show any marked differences. There was no significant change in VCI, FIR or FI. In summary, the VAD, VSD and VPI were all distinctively decreased, indicating that the blood flow area and the number of blood vessels decreased at the same time. Under this circumstance, the increase in VDI was more likely to represent the decrease in the numbers of vessels with a relatively small caliber, also known as a closure of these vessels. In the SCP, the superior and nasal peripapillary areas are the quadrants most vulnerable to vessel density change. The normal morphology of vessels, the flow impairment size and the flow of the SCP were not affected in this study.

In the DCP, most peripapillary blood circulation indices significantly changed at follow-up compared with the baseline (Table 3). The VDI showed a tendency to decrease. The VDI of the overall, inferior and temporal regions significantly decreased, indicating that the average vessel caliber decreased in these areas. There was no significant change in the VDI of other quadrants. The VAD showed a tendency to decrease. The VAD significantly decreased in all quadrants except the nasal quadrant, indicating that these areas had a smaller blood flow area. The VSD showed a tendency to decrease. The VSD of all quadrants decreased significantly, and the extent of the decrease was most distinctive in the temporal and nasal quadrants, indicating that the number of peripapillary blood vessels dropped. The VPI also showed a tendency to decrease. The VPI of the superior, nasal and temporal quadrants decreased significantly, indicating that there was a decrease in the blood flow area in these quadrants. The VPI of the inferior quadrant did not show a distinct

Table 2
The peripapillary blood circulation indices in the superficial capillary plexus in 2019 and 2021.

Parameters	2019	2021	Change Rate	*t* value	*P* value
Vessel Diameter Index (VDI)					
Overall	23.07 ± 0.41	23.12 ± 0.29	0.19%	0.8	0.4274
Nasal	23.11 ± 0.45	23.31 ± 0.42	0.89%	2.32	0.0277
Superior	23.35 ± 0.39	23.54 ± 0.59	0.78%	1.97	0.0582
Temporal	23.73 ± 0.60	23.73 ± 0.52	0.01%	0.02	0.9812
Inferior	23.37 ± 0.36	23.59 ± 0.61	0.94%	2.65	0.0130
Vessel Area Density (VAD)					
Overall	0.57 ± 0.17	0.57 ± 0.38	−0.61%	−1.07	0.2955
Nasal	0.59 ± 0.03	0.58 ± 0.02	−0.88%	−1.01	0.32
Superior	0.64 ± 0.02	0.63 ± 0.02	−1.88%	−3.18	0.0035
Temporal	0.60 ± 0.02	0.59 ± 0.02	−1.01%	−1.53	0.1375
Inferior	0.63 ± 0.02	0.62 ± 0.02	−1.02%	−1.6	0.1205
Vessel Skeleton Density (VSD)					
Overall	0.14 ± 0.00	0.14 ± 0.02	−0.81%	−1.53	0.1364
Nasal	0.15 ± 0.01	0.14 ± 0.00	−1.85%	−2.61	0.0143
Superior	0.16 ± 0.01	0.15 ± 0.01	−2.64%	−6.96	<0.0001
Temporal	0.15 ± 0.00	0.15 ± 0.00	−1.14%	−2	0.0547
Inferior	0.16 ± 0.01	0.15 ± 0.00	−1.80%	−3.09	0.0044
Vessel Perimeter Index (VPI)					
Overall	0.31 ± 0.01	0.31 ± 0.00	0.12%	0.27	0.789
Nasal	0.33 ± 0.01	0.32 ± 0.01	−0.92%	−2.15	0.0397
Superior	0.33 ± 0.00	0.31 ± 0.01	−1.05%	−4.9	<0.0001
Temporal	0.32 ± 0.01	0.32 ± 0.00	−0.66%	−1.74	0.0925
Inferior	0.33 ± 0.00	0.33 ± 0.01	−0.47%	−1.1	0.2823
Vessel Complexity Index (VCI)					
Overall	15175055186 ± 457352042	15305346763 ± 403929897	0.86%	1.81	0.0815
Nasal	2052.42 ± 101.28	2052.33 ± 66.55	0.00%	−0.01	0.9956
Superior	1946.04 ± 76.62	1948.03 ± 54.86	0.10%	0.17	0.8696
Temporal	1912.90 ± 79.33	1910.93 ± 80.29	−0.10%	−0.17	0.8637
Inferior	1903.32 ± 103.56	1931.99 ± 56.75	1.51%	1.29	0.2068
Flux Index (FI)					
Overall	0.30 ± 0.02	0.30 ± 0.02	0.18%	0.16	0.8752
Nasal	0.50 ± 0.04	0.51 ± 0.05	2.36%	1.38	0.1792
Superior	0.59 ± 0.03	0.58 ± 0.03	−0.87%	−0.85	0.4017
Temporal	0.53 ± 0.03	0.54 ± 0.04	1.31%	1.11	0.2751
Inferior	0.58 ± 0.03	0.58 ± 0.04	0.01%	0.01	0.9953
Flow Impairment Region (FIR)					
Overall	0.45 ± 0.12	0.24 ± 0.03	−44.71%	−1.49	0.1461
Nasal	0.07 ± 0.05	0.08 ± 0.05	12.79%	0.85	0.3998
Superior	0.03 ± 0.01	0.03 ± 0.02	5.68%	0.49	0.6307
Temporal	0.06 ± 0.04	0.05 ± 0.04	−7.14%	−0.65	0.5218
Inferior	0.09 ± 0.02	0.05 ± 0.04	−50.20%	−1.19	0.244

Change rate= (values in 2021- values in 2019)/values in 2019.

difference. The VCI showed a tendency to increase. The VCI of the overall peripapillary region and the superior quadrant significantly increased, indicating that the vessel morphology and tortuosity of these regions worsened. The VCI of other quadrants did not show a distinct change. The FIR showed a tendency to increase. The FIR of the superior quadrant significantly increased, indicating that the size of the flow impairment area was largest in the superior quadrant. Other quadrants did not show a significant change. The FI showed a tendency to decrease. The FI values of the superior, temporal and inferior quadrants significantly decreased, indicating that the blood flow was considerably reduced. As a whole, blood circulation indices including the VDI, the VAD, the VSD, the VPI and the FI decreased, and the blood circulation indices represent the abnormalities of microcirculation and microvasculature including the FIR and the VCI increased. This finding indicates that the average vessel caliber, total blood flow area, total vessel quantity and blood flow significantly dropped, while the vessel abnormalities and flow impairment region deteriorated. When the VAD, the VSD and the VPI decreased, the decrease in the VDI was more likely to be a shrinking of blood vessels rather than a closure of them. Unlike the SCP, the superior and inferior quadrants of the DCP were more vulnerable and affected.

In the correlation analysis of the relative changes in blood circulation indices in the SCP, no significant relevant factors were revealed (not shown in the results); therefore, no further regression analysis was performed. The correlation analysis of the blood circulation index change ratios in DCP revealed age, diabetes duration, height growth, change in glycosylated hemoglobin and the corresponding baseline blood circulation indices as significant relevant factors. The significantly altered relative changes in blood circulation indices were used as dependent variables, and the abovementioned meaningful relevant factors were used as independent variables. All positive results and some negative results of the multiple regression analysis are shown in Table 4. In addition, a multiple regression analysis that included the relative changes in the VD (nasal), VAD (overall, superior, nasal, inferior), VSD (overall, nasal, temporal), VPI (nasal, superior, temporal), VCI (overall) and FI (superior, temporal) as dependent variables also failed to reveal any significant relevant factors (not shown in the results). Multiple regression revealed that height growth was an independent influence on inferior VAD, inferior VSD and inferior FI ($\beta = -0.6071$, $P = 0.0411$; $\beta = -0.6666$, $P = 0.0209$; $\beta = -0.6711$, $P = 0.0324$); the greater the height growth in the preceding 2 years, the lower the VAD, VSD and FI were in 2021. The duration of diabetes was an independent factor influencing the inferior VCI and superior FIR ($\beta = -0.1751$, $P = 0.00317$; $\beta = -0.4766$, $P = 0.0231$); the longer the DM duration was, the larger the VCI and FIR were when the follow-up period ended. The change in the glycosylated hemoglobin percentage (HbA1c%) value was an independent factor influencing the superior FIR; the higher the HbA1c% value at follow-up, the larger the FIR was in 2021.

Table 3
The peripapillary blood circulation indices in the deep capillary plexus in 2019 and 2021.

Parameters	2019	2021	Change Rate	*t* value	*P* value
Vessel Diameter Index (VDI)					
Overall	21.29 ± 0.04	21.05 ± 0.04	−1.13%	−3.5	0.0015
Nasal	21.19 ± 0.71	21.40 ± 0.07	1.00%	1.39	0.1738
Superior	21.20 ± 0.57	21.05 ± 0.59	−0.70%	−1.27	0.2148
Temporal	21.79 ± 0.53	21.59 ± 0.53	−0.94%	−2.39	0.0235
Inferior	21.80 ± 0.58	21.60 ± 0.52	−0.91%	−2.07	0.0470
Vessel Area Density (VAD)					
Overall	0.49 ± 0.02	0.47 ± 0.20	−3.65%	−3.77	0.0007
Nasal	0.49 ± 0.04	0.48 ± 0.04	−2.70%	−1.59	0.1231
Superior	0.51 ± 0.04	0.49 ± 0.03	−4.13%	−3.4	0.0020
Temporal	0.53 ± 0.03	0.50 ± 0.02	−4.58%	−5.11	<0.0001
Inferior	0.52 ± 0.03	0.50 ± 0.02	−3.93%	−5.02	<0.0001
Vessel Skeleton Density (VSD)					
Overall	0.13 ± 0.00	0.13 ± 0.00	−2.56%	−3.24	0.0030
Nasal	0.14 ± 0.00	0.13 ± 0.00	−3.62%	−2.77	0.0097
Superior	0.14 ± 0.00	0.14 ± 0.00	−3.42%	−3.99	0.0004
Temporal	0.14 ± 0.01	0.14 ± 0.00	−3.63%	−4.97	<0.0001
Inferior	0.14 ± 0.01	0.14 ± 0.00	−2.68%	−4.65	<0.0001
Vessel Perimeter Index (VPI)					
Overall	0.31 ± 0.01	0.30 ± 0.01	−1.11%	−1.64	0.1114
Nasal	0.31 ± 0.01	0.31 ± 0.02	−2.57%	−2.55	0.0163
Superior	0.32 ± 0.01	0.31 ± 0.01	−2.00%	−3.16	0.0037
Temporal	0.32 ± 0.01	0.32 ± 0.01	−2.06%	−3.98	0.0004
Inferior	0.31 ± 0.01	0.31 ± 0.01	−0.82%	−1.69	0.1026
Vessel Complexity Index (VCI)					
Overall	16947477493 ± 671908782	17197898864 ± 434075066	1.48%	2.37	0.0248
Nasal	2256.07 ± 93.88	2220.62 ± 97.45	−1.57%	−2.03	0.0521
Superior	2247.50 ± 77.44	2256.21 ± 72.40	0.39%	0.61	0.5444
Temporal	2185.96 ± 106.66	2193.57 ± 103.77	0.35%	0.57	0.5745
Inferior	2106.35 ± 212.11	2195.23 ± 70.28	4.22%	2.31	0.0280
Flux Index (FI)					
Overall	0.18 ± 0.02	0.16 ± 0.01	−9.28%	−5.3	<0.0001
Nasal	0.33 ± 0.03	0.33 ± 0.03	−1.39%	−0.65	0.5228
Superior	0.36 ± 0.04	0.34 ± 0.03	−6.36%	−4.33	0.0002
Temporal	0.37 ± 0.03	0.35 ± 0.03	−5.89%	−5.3	<0.0001
Inferior	0.40 ± 0.03	0.37 ± 0.03	−6.46%	−5.8	<0.0001
Flow Impairment Region (FIR)					
Overall	1.37 ± 1.28	1.61 ± 0.57	17.80%	0.75	0.4610
Nasal	0.24 ± 0.33	0.36 ± 0.54	49.15%	1.22	0.2332
Superior	0.09 ± 0.11	0.16 ± 0.18	83.77%	2.49	0.0187
Temporal	0.09 ± 0.06	0.12 ± 0.09	32.03%	1.99	0.0557
Inferior	0.20 ± 0.39	0.12 ± 0.11	−38.99%	−1.19	0.2433

Change rate= (values in 2021- values in 2019)/values in 2019.

Table 4
Multiple regression analyses of the blood circulation indices in the deep capillary plexus.

Deep Capillary Plexus	Variables	Intercept	Baseline value in 2019	Age in 2021	DM duration in 2021	ΔHeight	ΔHbA1c	*F* value, *P* value
VDI Overall	*β* coefficient	0	−0.3929	−0.1511	0.0256	−0.1135	0.3681	1.81, 0.1683
	P value	0.0925	0.0880	0.6522	0.9149	0.7322	0.1173	
VAD Inferior	*β* coefficient	0	−0.5575	−0.4116	0.0889	−0.6071	0.2304	4.02, 0.0149
	P value	0.0087	0.0073	0.1509	0.667	0.0411	0.2107	
VSD Inferior	*β* coefficient	0	−0.647	−0.484	−0.0265	−0.6666	0.0984	4.68, 0.0080
	P value	0.0013	0.0019	0.0799	0.8963	0.0209	0.5673	
VPI Superior	*β* coefficient	0	−0.6261	−0.3221	0.2966	0.0057	0.0339	3.53, 0.0243
	P value	0.0254	0.0183	0.2736	0.173	0.9842	0.8779	
VCI Inferior	*β* coefficient	0	−0.9213	0.1052	−0.1751	−0.0463	0.0873	48.74, <0.0001
	P value	<0.0001	<0.0001	0.3429	0.0317	0.6807	0.2277	
FI Inferior	*β* coefficient	0	−0.3971	−0.5044	0.3051	−0.6711	0.2108	3.78, 0.01880
	P value	0.0661	0.0557	0.0927	0.1739	0.0324	0.2563	
FIR Superior	*β* coefficient	0	−0.2597	0.3022	−0.4766	−0.2287	−0.4326	4.36, 0.0107
	P value	0.6831	0.1614	0.2743	0.0231	0.4046	0.0244	

VDI= Vessel Diameter Index, VAD= Vessel Area Density, VSD= Vessel Skeleton Density, VPI= Vessel Perimeter Index, VCI= Vessel Complexity Index, FI= Flux Index, FIR= Flow Impairment Region. ΔHeight = Height in 2021-Height in 2019. ΔHbA1c (hemoglobin A1c, HbA1c) = HbA1c in 2021- HbA1c in 2019.

4. Discussion

In a PubMed search, we failed to discover any prior studies focused on the longitudinal alterations of the peripapillary blood circulation indices among T1DM children without DR. This study revealed that the only change in SCP blood flow after 2 years was a decrease in vessel density. The vessel density, blood flow, vessel morphological abnormalities and flow impairment area all deteriorated in the DCP over the follow-up period, and the factors influencing these changes were height growth, change in HbA1c% and duration of diabetes. Where previous cross-sectional studies merely conjectured, this longitudinal observational study confirmed that microcirculation and microvasculature impairment

emerged in the DCP earlier than in the SCP - that is, the peripapillary DCP is more susceptible and vulnerable to DR progression than the SCP in the early stage of preclinical DR and could be used as a target for DR screening. Along with blood glucose control and duration of diabetes, more attention should also be paid to the unique manifestations of DR among diabetic children during growth and puberty.

DR is a class of diseases mainly characterized by alteration, degeneration and destruction of capillaries. In DM patients, blood glucose levels remain high for long periods, and advanced glycation end-products accumulate in retinal vasculature, inducing apoptosis of pericytes, thickening of the vessel basement membrane and hyperplasia of the endothelium; these changes eventually reduce the permeability of capillaries and reduce the vessel density.[17] Before the advent of any clinical signs of DR, the abovementioned alterations are already in progress. Thus, the blood circulation indices significantly deteriorated among the T1DM children without DR in this longitudinal observational study and previous cross-sectional studies.[10,11,18–20] However, the emergence of evidence of neurodegeneration among DR patients has provided a new reason for this phenomenon. It is widely believed that neurodegeneration induces apoptosis of neurons and dysfunction of glial cells, which degrades the blood–retina barrier and neurovascular coupling and eventually leads to microvascular dysfunction in preclinical DR.[5–7] In 2018, Zhang[9] et al. determined that the reduction of peripapillary vessel density precedes the reduction of RNFL thickness. Zhang also speculated that peripapillary microcirculation impairment precipitates the metabolic dysfunction of neurons, which impels the progression of DR. We infer that there may be a reciprocal causal relationship between microvasculature impairment and neurodegeneration. On the one hand, impaired microcirculation induces the dysfunction of neurons; on the other hand, neurodegeneration aggravates microvascular dysfunction. In summary, these two factors form a vicious cycle that drives the progression of DR. Hence, it is very meaningful to observe long-term alterations in peripapillary blood flow. These changes can reflect not only the extent of peripapillary microvascular impairment but also the blood and oxygen supply of the optic nerve head.

After two years, the vessel density of the SCP's superior and nasal quadrants distinctively decreased. The temporal quadrant had no obvious alteration. In their study, Guven[11] et al. observed that children with T1DM exhibited lower vessel density in the optic disc area. Contrarily, Pilotto[21] et al. reported an increase in peripapillary capillary vessel density in T1DM children compared to healthy controls. Koca[20] et al., however, found no significant difference in peripapillary capillary vessel density between T1DM children and control groups. Our research group's previous cross-sectional study also did not identify any notable differences in superficial peripapillary microvasculature among T1DM children without DR compared to healthy counterparts. However, it is crucial to note that Pilotto and Koca's analyses focused on the radial peripapillary capillary plexus (RPC), encompassing the inner limiting membrane and the RNFL. Beyond the RPC, the SCP also includes the ganglion cell layer and inner plexiform layer. The discrepancies in these cross-sectional studies' conclusions may stem from variations in diabetes duration and disease progression. Specifically, the mean age of Pilotto's study subgroup without DR was 17.2 years, with a diabetes duration averaging 12.5 years – significantly longer than the approximate 5-year duration noted in other studies. This disparity underscores the necessity for longitudinal studies to further clarify these observations. Our 2-year follow-up study within the SCP framework corroborates that peripapillary vessel density reduction also occurs in T1DM children without DR. Our findings suggest that initially, peripapillary blood flow in children with T1DM does not differ from the normal population before the onset of diabetic retinopathy, but subsequently begins to decrease markedly. Peripapillary vessel density was considered to be relevant to the RNFL thickness.[6] Our research group's study among T1DM children revealed that the thinning of the RNFL thickness in nasal quadrants preceded that in other quadrants.[22] The above studies provided strong support. In particular, the VAD, VSD and VPI all decreased in the SCP, while the VDI increased. When the blood flow area and vessel quantity all declined, the only reason for the increase in average vessel caliber was the closure of vessels with lesser caliber. This phenomenon was in accord with the pathophysiological characteristic of DR for violating small vessels and capillaries.[17] Although the peripapillary vessel density in the SCP was decreased, the FI, FIR and VCI were not influenced, indicating that the blood supply was not severely affected.

In the DCP, observations revealed not only dramatic reductions in the blood flow area and the number of vessels but also distinct deteriorations in the blood flow, flow impairment region and vessel morphology, indicating that the blood supply and oxygen supply were severely restricted. The deep retina tissue has a high metabolic demand and relatively low perfusion and is susceptible to the metabolic pressure induced by DM.[23] The injury in the DCP microcirculation always precedes the SCP, and the extent of the DCP microvascular impairment was consistent with DR progression.[24] The central retinal artery (CRA) divides into 4 branches, namely, the superior nasal, superior temporal, inferior nasal and inferior temporal branches. These 4 arterioles course through the RNFL and give off collateral branches that dive deeper through the retinal layers and comprise two major capillary networks within their respective quadrants: the inner capillary network within the ganglion cell layer and the outer capillary network within the inner nuclear layer.[25] The SCP in this study comprised the arterioles in the RNFL and the inner capillary network, while the DCP comprised only the outer capillary network. The outer capillary network is the most vulnerable vasculature in the retina and cannot be repaired.[26–28] There was also a decrease in vessel density in the DCP among high myopia and glaucoma patients.[23,29] The above mechanisms provided strong support for badly impaired DCP and slightly affected SCP in this study from all aspects. First, the SCP contains terminal arterioles of the CRA, while the DCP contains only capillaries. DR tends to violate microvasculature and capillaries. Second, the DCP is more vulnerable and susceptible. In contrast to what was observed in the SCP, the inferior, superior and temporal quadrants were the most affected areas of the DCP. However, the existing data provide limited confirmation of this interpretation.

In the regression analysis, height growth during the follow-up period was an independent influencing factor of inferior VAD, VSD and FI. The greater the height growth, the worse the blood circulation indices were. The participants in this study were in the growth and puberty period, and the average height in 2021 (1.57 ± 0.13) was significantly higher than that in 2019 (1.47 ± 0.17). However, we failed to discover any relevance between height growth and DR progression or vessel density decrease among DM patients in previous research. We presume that great growth demands in children may exacerbate any existing impairment of peripapillary microcirculation. Unlike older DM patients, who are physiologically mature, the pediatric DM patients in this study had not yet completed puberty. High blood glucose hinders normal growth in children,[30,31] while strong growth needs may aggravate the progression of DM complications. In the future, we should think highly of the problem of reconciling maintaining normal growth with slowing down DM complication progression among children with DM. DM duration was an independent influencing factor of inferior VCI. It was harder to maintain normal vessel morphology as the duration of diabetes increased, which conformed to previous studies.[32] The change in HbA1c% was an independent influencing factor of superior FIR; the more severe the HbA1c% change was, the larger the flow impairment area. Glycosylated hemoglobin reflected the average blood glucose level in the past 3 months, and the HbA1c% level in 2021 (7.91 ± 1.54) was significantly higher than that in 2019 (7.08 ± 1.76). Blood glucose levels are highly relevant to microvasculature damage.[17,33] Although the difference in HbA1c% levels between the two timepoints is only a crude reflection of average blood glucose during the follow-up period, it could provide information on the effects of behavioral change and externally imposed interventions on children's blood glucose control.

Currently, studies concentrating on peripapillary OCTA usually use the 4.5 mm * 4.5 mm optic nerve head scan mode and analyze the RPC.

This study used the 6 mm * 6 mm angiography scan mode and analyzed the SCP and DCP. It is not convenient to directly compare our results from other studies with regular scan and analysis modes. However, a larger scan size and larger analysis range could provide more information. This study should have reported the macular blood circulation index alterations at the same time, as there are already plentiful data that cover only the peripapillary area. In addition, this study failed to acquire the follow-up data of normal children due to their poor compliance. Unfortunately, we could not compare the longitudinal peripapillary blood flow index changes between normal children and T1DM children. In addition, a longer follow-up duration and a larger cohort size are likely to yield more comprehensive information.

In summary, this study observed longitudinal peripapillary blood circulation index changes for 2 years among T1DM children without visual impairment and DR who were still in puberty. We revealed that the vessel density of the peripapillary SCP decreased. The vessel density, blood flow, vessel morphological abnormalities and flow impairment area all deteriorated in the DCP. The height growth, change in HbA1c% level and DM duration were independent factors influencing the relative change in blood circulation indices in the DCP. Therefore, future studies on DR prevention and progression should pay more attention to the importance and susceptibility of peripapillary DCP and the unique characteristic of DR progression among DM patients in puberty.

Study approval

This study was performed in line with the principles of the Declaration of Helsinki. Approval was granted by the Ethics Committee of Shanghai General Hospital (approval number 2018KY209) and the Children's Hospital affiliated with Fudan University in Shanghai (approval number: 012018).

Author contributions

All authors contributed to the study conception and design. Material preparation, data collection and analysis were performed by LC, CY, and HZ. The first draft of the manuscript was written by LC, HZ and all authors commented on previous versions of the manuscript. All authors read and approved the final manuscript.

Funding

This study was supported by Chinese National key research and development program (Project number 2021YFC2702100) and Shanghai engineering research center of precise diagnosis and treatment of eye diseases, Shanghai, China (Project No. 19DZ2250100).

Declaration of competing interest

The authors declare that they have no known competing financial interests or personal relationships that could have appeared to influence the work reported in this paper.

Acknowledgments

Thanks to all the peer reviewers for their opinions and suggestions.

Abbreviations

T1DM	Type 1 diabetes mellitus
DR	Diabetic retinopathy
RNFL	Retinal nerve fiber layer
OCTA	Ooptical coherence tomography angiography
OMAG	Optical microangiography algorithm
SCP	Superficial capillary plexus
DCP	Deep capillary plexus
VDI	Vessel diameter index
VAD	Vessel area density
VSD	Vessel skeleton density
VPI	Vessel perimeter index
VCI	Vessel complexity index
FIR	Flow impairment region
FI	Flux index

References

1. Patterson C, Guariguata L, Dahlquist G, et al. Diabetes in the young - a global view and worldwide estimates of numbers of children with type 1 diabetes. *Diabetes Res Clin Pract*. 2014;103:161–175. https://doi.org/10.1016/j.diabres.2013.11.005.
2. Bourne RR, Stevens GA, White RA, et al. Causes of vision loss worldwide, 1990-2010: a systematic analysis. *Lancet Global Health*. 2013;1:e339–e349. https://doi.org/10.1016/s2214-109x(13)70113-x.
3. Forbes JM, Cooper ME. Mechanisms of diabetic complications. *Physiol Rev*. 2013;93:137–188. https://doi.org/10.1152/physrev.00045.2011.
4. Scanlon PH, Aldington SJ, Stratton IM. Epidemiological issues in diabetic retinopathy. *Middle East Afr J Ophthalmol*. 2013;20:293–300. https://doi.org/10.4103/0974-9233.120007.
5. Simó R, Stitt AW, Gardner TW. Neurodegeneration in diabetic retinopathy: does it really matter? *Diabetologia*. 2018;61:1902–1912. https://doi.org/10.1007/s00125-018-4692-1.
6. Lim HB, Shin YI, Lee MW, et al. Longitudinal changes in the peripapillary retinal nerve fiber layer thickness of patients with type 2 diabetes. *JAMA Ophthalmol*. 2019;137:1125–1132. https://doi.org/10.1001/jamaophthalmol.2019.2537.
7. Simó R, Hernández C. Neurodegeneration in the diabetic eye: new insights and therapeutic perspectives. *Trends Endocrinol Metabol*. 2014;25:23–33. https://doi.org/10.1016/j.tem.2013.09.005.
8. Chen X, Nie C, Gong Y, et al. Peripapillary retinal nerve fiber layer changes in preclinical diabetic retinopathy: a meta-analysis. *PLoS One*. 2015;10:e0125919. https://doi.org/10.1371/journal.pone.0125919.
9. Cao D, Yang D, Yu H, et al. Optic nerve head perfusion changes preceding peripapillary retinal nerve fibre layer thinning in preclinical diabetic retinopathy. *Clin Exp Ophthalmol*. 2019;47:219–225. https://doi.org/10.1111/ceo.13390.
10. Zhang B, Chou Y, Zhao X, et al. Early detection of microvascular impairments with optical coherence tomography angiography in diabetic patients without clinical retinopathy: a meta-analysis. *Am J Ophthalmol*. 2021;222:226–237. https://doi.org/10.1016/j.ajo.2020.09.032.
11. Demir ST, Ucar A, Elitok GK, et al. Evaluation of retinal neurovascular structures by optical coherence tomography and optical coherence tomography angiography in children and adolescents with type 1 diabetes mellitus without clinical sign of diabetic retinopathy. *Graefes Arch Clin Exp Ophthalmol*. 2020;258:2363–2372. https://doi.org/10.1007/s00417-020-04842-1.
12. Li T, Jia Y, Wang S, et al. Retinal microvascular abnormalities in children with type 1 diabetes mellitus without visual impairment or diabetic retinopathy. *Invest Ophthalmol Vis Sci*. 2019;60:990–998. https://doi.org/10.1167/iovs.18-25499.
13. Laíns I, Wang JC, Cui Y, et al. Retinal applications of swept source optical coherence tomography (OCT) and optical coherence tomography angiography (OCTA). *Prog Retin Eye Res*. 2021;84:100951. https://doi.org/10.1016/j.preteyeres.2021.100951.
14. Zhao Q, Yang WL, Wang XN, et al. Repeatability and reproducibility of quantitative assessment of the retinal microvasculature using optical coherence tomography angiography based on optical microangiography. *Biomed Environ Sci*. 2018;31:407–412. https://doi.org/10.3967/bes2018.054.
15. Agiostratidou G, Anhalt H, Ball D, et al. Standardizing clinically meaningful outcome measures beyond HbA(1c) for type 1 diabetes: a consensus report of the American association of clinical endocrinologists, the American association of diabetes educators, the American diabetes association, the endocrine society, JDRF international, the leona M. and harry B. Helmsley charitable trust, the pediatric endocrine society, and the T1D exchange. *Diabetes Care*. 2017;40:1622–1630. https://doi.org/10.2337/dc17-1624.
16. Petersmann A, Müller-Wieland D, Müller UA, et al. Definition, classification and diagnosis of diabetes mellitus. *Exp Clin Endocrinol Diabetes*. 2019;127:S1–s7. https://doi.org/10.1055/a-1018-9078.
17. Roy S, Kern TS, Song B, et al. Mechanistic insights into pathological changes in the diabetic retina: implications for targeting diabetic retinopathy. *Am J Pathol*. 2017;187:9–19. https://doi.org/10.1016/j.ajpath.2016.08.022.
18. Inanc M, Tekin K, Kiziltoprak H, et al. Changes in retinal microcirculation precede the clinical onset of diabetic retinopathy in children with type 1 diabetes mellitus. *Am J Ophthalmol*. 2019;207:37–44. https://doi.org/10.1016/j.ajo.2019.04.011.
19. Sacconi R, Casaluci M, Borrelli E, et al. Multimodal imaging assessment of vascular and neurodegenerative retinal alterations in type 1 diabetic patients without fundoscopic signs of diabetic retinopathy. *J Clin Med*. 2019;8. https://doi.org/10.3390/jcm8091409.
20. Sousa DC, Leal I, Moreira S, et al. Optical coherence tomography angiography study of the retinal vascular plexuses in type 1 diabetes without retinopathy. *Eye*. 2020;34:307–311. https://doi.org/10.1038/s41433-019-0513-0.
21. Pilotto E, Torresin T, Leonardi F, et al. Retinal microvascular and neuronal changes are also present, even if differently, in adolescents with type 1 diabetes without clinical diabetic retinopathy. *J Clin Med*. 2022;11. https://doi.org/10.3390/jcm11143982.

22. Yu Q, Xiao Y, Lin Q, et al. Two-year longitudinal study on changes in thickness of the retinal nerve fiber layer and ganglion cell layer in children with type 1 diabetes mellitus without visual impairment or diabetic retinopathy. *Curr Eye Res*. 2022;47:1218–1225. https://doi.org/10.1080/02713683.2022.2079142.
23. Ye J, Wang M, Shen M, et al. Deep retinal capillary plexus decreasing correlated with the outer retinal layer alteration and visual acuity impairment in pathological myopia. *Invest Ophthalmol Vis Sci*. 2020;61:45. https://doi.org/10.1167/iovs.61.4.45.
24. Onishi AC, Nesper PL, Roberts PK, et al. Importance of considering the middle capillary plexus on OCT angiography in diabetic retinopathy. *Invest Ophthalmol Vis Sci*. 2018;59:2167–2176. https://doi.org/10.1167/iovs.17-23304.
25. Standring S. Gray's Anatomy (41tst ed.). Edinburgh: Elsevier Churchill Livingstone. doi..
26. Balaratnasingam C, An D, Sakurada Y, et al. Comparisons between histology and optical coherence tomography angiography of the periarterial capillary-free zone. *Am J Ophthalmol*. 2018;189:55–64. https://doi.org/10.1016/j.ajo.2018.02.007.
27. Bek T. Transretinal histopathological changes in capillary-free areas of diabetic retinopathy. *Acta Ophthalmol*. 1994;72:409–415. https://doi.org/10.1111/j.1755-3768.1994.tb02787.x.
28. Moore J, Bagley S, Ireland G, et al. Three dimensional analysis of microaneurysms in the human diabetic retina. *J Anat*. 1999;194(Pt 1):89–100. https://doi.org/10.1046/j.1469-7580.1999.19410089.x.
29. Wang YX, Panda-Jonas S, Jonas JB. Optic nerve head anatomy in myopia and glaucoma, including parapapillary zones alpha, beta, gamma and delta: histology and clinical features. *Prog Retin Eye Res*. 2021;83:100933. https://doi.org/10.1016/j.preteyeres.2020.100933.
30. Shpitzer H, Lazar L, Shalitin S, et al. Good glycemic control at puberty in boys with type 1 diabetes is important for final height. *J Diabetes*. 2021;13:998–1006. https://doi.org/10.1111/1753-0407.13214.
31. Parente EB, Harjutsalo V, Forsblom C, et al. Waist-height ratio and the risk of severe diabetic eye disease in type 1 diabetes: a 15-year cohort study. *J Clin Endocrinol Metab*. 2022;107:e653–e662. https://doi.org/10.1210/clinem/dgab671.
32. Chen L, Magliano DJ, Zimmet PZ. The worldwide epidemiology of type 2 diabetes mellitus–present and future perspectives. *Nat Rev Endocrinol*. 2011;8:228–236. https://doi.org/10.1038/nrendo.2011.183.
33. Wurm M, Kuhnemund L, Maier L, et al. Hemoglobin A1c and retinal arteriolar narrowing in children with type 1 diabetes: the diagnostics of early atherosclerosis risk in kids study. *Pediatr Diabetes*. 2019;20:622–628. https://doi.org/10.1111/pedi.12858.

Lipu Cui
Department of Ophthalmology, Shanghai General Hospital, Shanghai Jiao Tong University School of Medicine, Shanghai, China

Chenhao Yang[**]
Department of Ophthalmology, Children's Hospital of Fudan University, Shanghai, China

Haidong Zou[*]
Department of Ophthalmology, Shanghai General Hospital, Shanghai Jiao Tong University School of Medicine, Shanghai, China
Shanghai Eye Diseases Prevention & Treatment Center, Shanghai Eye Hospital, Shanghai, China
Shanghai Key Laboratory of Fundus Diseases, Shanghai, China
National Clinical Research Center for Eye Diseases, Shanghai, China
Shanghai Engineering Center for Precise Diagnosis and Treatment of Eye Diseases, Shanghai, China

[**] Corresponding author. Children's Hospital of Fudan University, No. 399 Wanyuan Road, Shanghai, 201102, China.

[*] Corresponding author. Department of Ophthalmology, Shanghai General Hospital, Shanghai Jiao Tong University School of Medicine, Shanghai, China.
E-mail address: ychben@hotmail.com (C. Yang).
E-mail address: zouhaidong@sjtu.edu.cn (H. Zou).